Investigation of a Submerged Cavitating Jet Behaviour: Part One – The Phenomenon, Detection Technique and Sono-Luminesence

Ezddin Ali Farag Hutli
Ph.D. Student

Miloš S. Nedeljković
Professor

University of Belgrade
Faculty of Mechanical Engineering

In order to study and understand the jet structure and the behavior of cloud cavitation within time and space, visualization of highly submerged cavitating water jet has been done using 4-Quik-05 camera. This included obligatory synchronization technique and different types of lens-objectives. The influencing parameters, such as: injection pressure, downstream pressure and cavitation number were experimentally proven to be very significant. The recordings of sono-luminescence phenomenon proved the bubble collapse everywhere along the jet. In addition, the effect of temperature on sono-luminescence was a point of investigation .

Keywords: *Cavitating jet, cavitation cloud, cavitation ring, vapor cavity, cavitation number, sono-luminescence.*

1. INTRODUCTION

Flow visualization is an important tool in fluid dynamics research and it has been used extensively in the fields of engineering, physics, medical science, meteorology, oceanography, sport, aerodynamics, etc. Over the past few years, cavitating fluid jets have received a considerable attention, primarily with laboratory experiments, to understand their behaviour and to determine the feasibility of their use in a variety of situations. Recently, these testing and evaluation efforts have proven certain applications of cavitating jets, which include: cleaning paint and rust from metal surfaces; underwater removal of marine fouling; removing of high explosives from munitions; augmenting the action of deep-hole mechanical bits used to drill for petroleum or geothermal energy resources; wide use in cutting, penning and flushing. Thus cavitating fluid jet method is indeed commercially attractive, Soyama H et al. (1994), Vijay M et al. (1991) and Conn A et al. (1981).

Many researchers have made efforts to observe and to visualize the cavitating jet in order to understand its behavior, the mechanisms of formation of the cloud cavitation and stability of the characteristics of the cavitation.

Ganippa L. C et al. (2001), from their experimental results and observations using different nozzle inclinations (90, 85, 80 and 0 degree to the spray axis), indicate that the structure of cavitation and its distribution within the hole play a vital role in the spray pattern and atomization in the fuel injection system of the diesel engine and are very sensitive to the geometry of a sac and hole. In addition, in all four nozzles the inception bubbles grew intensively in the shear layer and developed into cloudlike coherent structures. Also, they found that the instabilities of the shear layer caused the cloud cavitation structures to break off, which subsequently led to the shedding of the cavitation cloud. In their case the shed cavitation was similar in shape to a horseshoe vortex.

Soyama H (2005) optimizes the cavitating jet in air, using high-speed photography observations. The result of the work reveals that the cavitating jet in air under high impact conditions shows periodic phenomena - the cavitation cloud in a low-speed water jet shedded periodically, the low-speed water jet had a wavy surface with a frequency related to that of the cloud shedding, the frequency of the wavy pattern of low-speed water jet decreased with increasing of the low-speed water jet injection pressure.

Soyama H et al. (1994, 1995) reported that the cavitation cloud shedding and the breakdown of the cloud of the cavitating jet in water took place periodically with a frequency in the range of 0.5 to 2 kHz. This frequency depends on the injection pressure of the cavitating jet and/or the cavitation number, but does not depend upon the nozzle geometry. Time period (interval) between one discharge and the next is scarcely dependent on nozzle geometry, but significantly on the injection pressure (direct proportion is stated). In addition, they reported that the break-off of the cloud could be related to time-dependent feature of the streamwise pressure gradient.

Keiichi, Yasuhiro (2002) investigated the cavitation inside the circular-cylindrical nozzle mounted in cavitation tunnel. They reported that the periodic shedding of a large scale vortex cavity exists in a transition cavitation stage from subcavitation to supercavitation state. This periodic shedding is dependent on formation and coalescence of micro-vortex cavities on the separated shear layer and the re-entrant motion after the shedding. In addition, they

Received: November 2007, Accepted: December 2007
Correspondence to: Dr Miloš Nedeljković
Faculty of Mechanical Engineering,
Kraljice Marije 16, 11120 Belgrade 35, Serbia
E-mail: mnedeljkovic@mas.bg.ac.yu

reported that the Strouhal number can be estimated from consideration of the motions of the vortex cavities on the separated shear layer and the re-entrant flow.

Kato H. et al. (1999) used laser holograph to observe and visualize the cavitation cloud on a foil. They visualized the U-shaped vortex cavitation surrounded by many bubbles and concluded that this is the main feature of their case of cavitation.

Toyoda K. et al. (1999) investigated the vortical structure of a circular water jet using a laser fluorescent dye and a laser light sheet. Their results of visualization show that the streamwise vortices have fundamental effect on the entrainment of ambient fluid.

In this paper visualization of high-submerged cavitating water jet was done using a 4-Quik-05 camera with synchronization technique and with different types of lens-objectives in order to study and understand the jet structure and the behavior of cloud cavitation within the time and space at certain hydrodynamic conditions.

2. EXPERIMENTAL SETUP AND MEASUREMENT PROCEDURE

The experimental setup for jet performance investigation is the closed hydraulic loop shown in Fig.1. High-speed submerged cavitating jet is produced in the test chamber by adjustment of appropriate hydrodynamic conditions and by final outflow to the test chamber through the nozzle. The specimens are mounted in the chamber co-axially with the nozzle, the chamber is filled-up with water, and then the water is pressurized by a plunger pump. Only one chamber is functional, while the other is for reserve. Valves with pressure gauge are used for pressure regulation in the system and water temperature is maintained within maximum 1°C of variation during the erosion tests by cooling circuit with the heat exchanger.

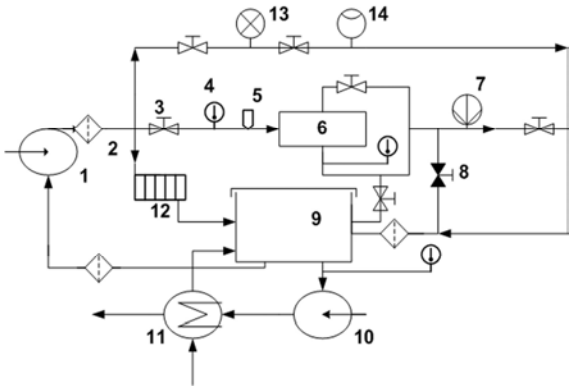

Figure 1. Schematic diagram of Cavitating jet machine. (1 - Plunger pump, 2 - Filter, 3 - Regulation valve, 4 – Temperature sensor, 5 - High-pressure transducer, 6 - Test chamber, 7 - Low pressure transducer, 8 - Safety valve, 9 - Tank, 10 - Circulation pump, 11 - Heat Exchanger, 12 - Energy dissipator, 13 - Pressure gauge, 14 - Flow indicator).

Test chamber is shown in Fig.2 (left). Hydrodynamic conditions were varied within the following limits: test chamber was 0.87 liters in volume and nozzles used were with diameters of 0.4, 0.45, 0.55 and 0.6 mm. The top speed of the jet is more than 200 m/s for upstream pressure set to 450 bar. The downstream pressure could be adjusted from atmospheric pressure up to 5 bar.

Jet impacts the sample S located $L = 25.67$ mm away from the nozzle (on the opposite side of the chamber – Fig. 2 (right). A rotating holder is used to attach up to 6 specimens (samples). This allows for switching from one sample to the other during the test. It also allows for quick start and/or stop of the exposure to cavitation without need for turning on/off of the test rig. The software used for data acquisition and control of the machine was LABVIEW 7.1.

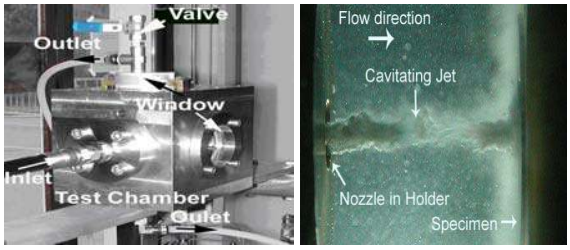

Figure 2. Left - Test chamber, Right - Cavitating jet impinging on the specimen.

Hydrodynamic conditions are settled-on to produce cavitating jet. The intensity of cavitating jet is controlled via upstream and downstream pressures, which are measured precisely by transducers and controlled using the needle valves (regulation valves). The filters are used to purify impurities from the circulating water. The temperature regulator and temperature sensors are used to control the water temperature. The nozzle may be mounted in the holder in two ways regarding the inlet and outlet diameters: with divergent and/or convergent conicity – Fig.3 shows holder and possible nozzle mountings.

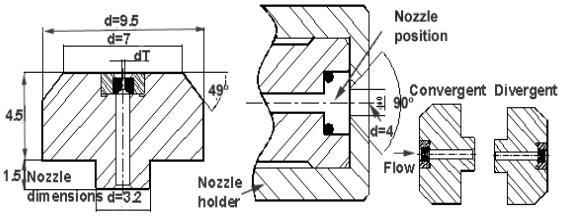

Figure 3. Nozzle geometry (dimensions mm), nozzle holder and two possible ways of mounting.

3. VISUALIZATION OF CAVITATING JETS USING 4-QUIK-05 CAMERA

The setup with Stanford Optics 4-QUIK-05 equipment through endoscopes with DRELLO 3244 flashlight stroboscope has been used for further visualization analysis. A personal computer equipped with a Matrox video card through a serial port controls the camera. A monitor was connected to the card for the real-time visualization of the results. The 4-Quick-05 camera is a special black-and-white CCD camera with light amplification (ICCD). Its special shutter permits exposure as short as 30 ns. The adjustable gain allows for operations with very low light, but then resolution drops as the gain is increased. Figs. 4 and 5 show the installation of the equipment.

3.1 Synchronization

Because of very rapid changes in the cavitation phenomenon within the order of μs, and in order to have enough light to illuminate the jet, the shutter and the flash discharge (Drello3244 and StrobexFlash CHADWICK) were synchronised using a photodiode in order to get enough light during the visulization. The photodiode was connected to an oscilloscope, which generates a TTL signal, used to trigger the camera shutter - Fig.4. A second oscilloscope is used to monitor the synchronism of the flash discharge and the trigger signal. Fig.6 shows the synchronization between the flash signal and the shutter signal.

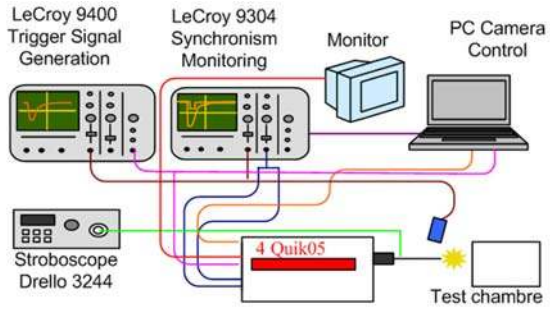

Figure 4. Scheme of the visualization system for synchronization process. The objective is the endoscope.

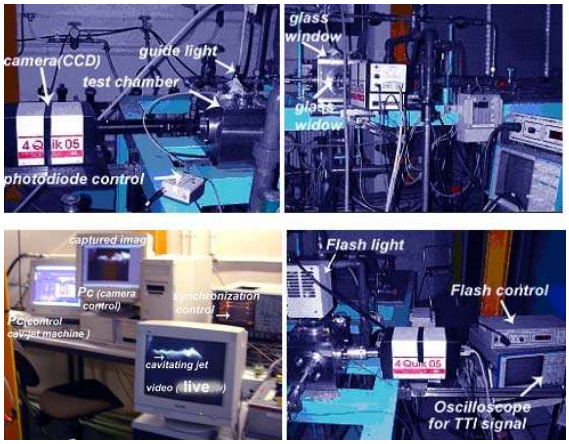

Figure 5. The images of instaallation of apparatus of the visualization system.

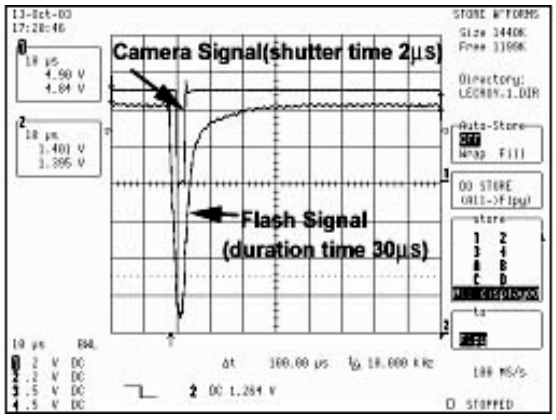

Figure 6. Picture from the Oscilloscope (LeCroy 9304) for camera and flash signals (Synchronization process).

3.2 Visualization of Cavitating Jet Using 4-Quik-05 Camera with Endoscope Objective

Pictures in Fig.8 were taken with the endoscope objective. The lens of the objective and the light flash lamp were mounted together in the same holder tube, as used in medicine investigations. This technique was used for two reasons: firstly, with intention to have the flashlight in the same window of visualization (in order to have a homogeneous light distribution in the test chamber and thus to enlight all jet parts with the same degree) and, secondly, to approach the window wall and the jet as close as possible. The objective has to be very near to the subject (in order of a few millimeters) for getting of the proper results.

The images in Fig.9 were obtained with 4 Quik 05 camera The objective used was Cosmicar television Lens 50 mm 1...14, the gain – 600 V and the shutter time - 1μs. From the group of images in Fig.9 we can note that the width of the jet is changeable with time of μs order and that the jet breaking point position is not at the same place in all images. The strong turbulences situation of the jet flow is the main reason for the points mentioned above. In addition, along the jet path hundred thousands of bubbles are collapsing, which leads to the change of pressure distribution in the test chamber - see Figs. 14 and 15.

In images of Fig.9 some parts of the jet reflected the flash light, but in general the upper part of the jet is brighter than the lower part. This is because the flash light was directed through the upper window. The rings are not the same in size, but this is normal because every picture represents a certain moment of jet life time. As it may be seen in the photos, the cavitating jet is changing with time in μs order (the same is also concluded in [2]).

3.3 Visualization of Cavitating Jet Using 4-Quik-05 Camera with Magnifier Lenses

In this part the objective with *magnifier lenses* was used in order to magnify the jet to get more information. In photos, the jet is divided into three parts which are overlapping one over each other as shown in Fig.7

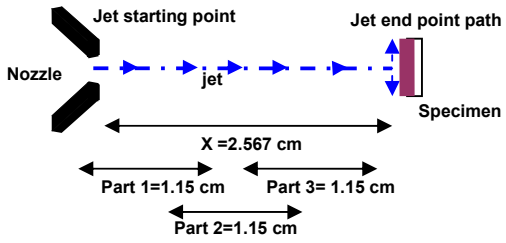

Figure 7. The manner dividing the cavitating jet during the visualization process using a magnifier objective.

The Navitar Digital Camera Adapter – Navitar's Zoom 6000 system (*Navitar 2x adapter (1-6010)(1-6030)(1-60135) magnifier lenses)* was used with 4-QUIK-05 camera and the flash light *chadwick-helmuth strobex* (duration time 30μs). Visualization has been

done two times, once with $p_2 = 0.77$ bar, $\sigma = 0.0063$ and once with $p_2 = 3.04$ bar, $\sigma = 0.025$, where cavitation number was calculated as $(\sigma = [(p_2 - p_v)/(0.5 \cdot \rho \cdot v_j^2)])$. The results are presented in Figs.10 and 11 respectively.

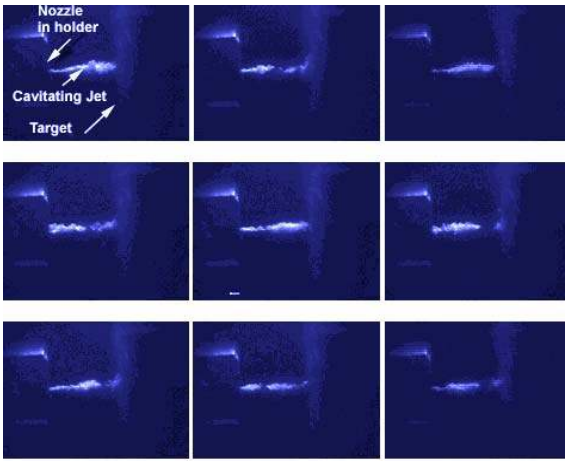

Figure 8. Images obtained with endoscope (Shutter time = 1μs, Gain = 600 V. Conditions: p_1=164 bar, p_2=0.77 bar, v_j=156 m/s, σ=0.0063, T =18°C).

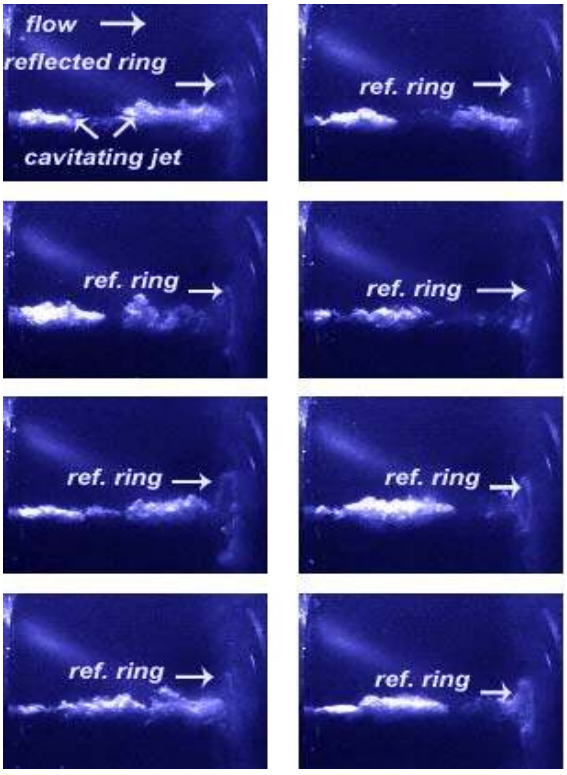

Figure 9. Images obtained by an objective Cosmicar television lens 50mm1...14. (Shutter time=1μs, Gain=600V. Conditions: p_1=147 bar, p_2=0.76 bar, v_j =148 m/s, σ=0.0069, T =18°C).

From all the images in Figs.10 and 11 (even though the resolution was not the best one), we can deduce that three parts of the jet are forming clusters or groups of bubbles which exist along the jet length. The jet surface in all images of three parts looks like rough surface. In some images the flash light was reflected (this happened when the light attacked on one or aog group of the sphere bubbles), and this is more clear in the images of the jet at $p_2 = 0.77$ bar, $\sigma = 0.0063$ than in other images. Also we can note that the jet width, jet penetration and the bubbles number increase as p_2 decreases. Quantity of bubbles can be deduced from the degree of reflecting light, where the images are brighter at lower values of p_2. It also means that the number of nonspherical bubbles at lower p_2 is higher than that in the case at higher p_2.

In the case of low p_2, where the jet can arrive the target wall and strikes it, it can be seen that at the first moment of striking the jet covers the entire target wall with a lot of bubbles which are distributed on whole the area of target wall. Immediately after the striking, the jet is reflected back and the rings appear in the images clearly. These rings contain a lot of bubbles, see Fig.13.

At high p_2 the jet can not arrive to the end of target distance. It is destroyed before the end of path, and the rings cannot be seen in this case. The repetition of the visualizations was done in order to improve the image quality by playing with the shutter time and the gain value to optimize the image resolution. For instance, hydrodynamic conditions for Figs.12 and 13 were not the same as for Figs.10 and 11.

4. SONO-LUMINESCENCE IN CAVITATING JET

The attempt to record the sono-luminescence (SL) phenomenon associated to the collapse of bubbles in cavitating jet was also done.The attempts were taken at different values of cavitation number $\sigma = 0.0125$, $\sigma = 0.0142$ and $\sigma = 0.0207$ at constant exit jet-velocity v_j and working fluid temperature T. Fig.14 shows representative frames with SL spots registered by the camera. In all shots of SL, the image contrast has been dramatically increased for the reasons of clarity.

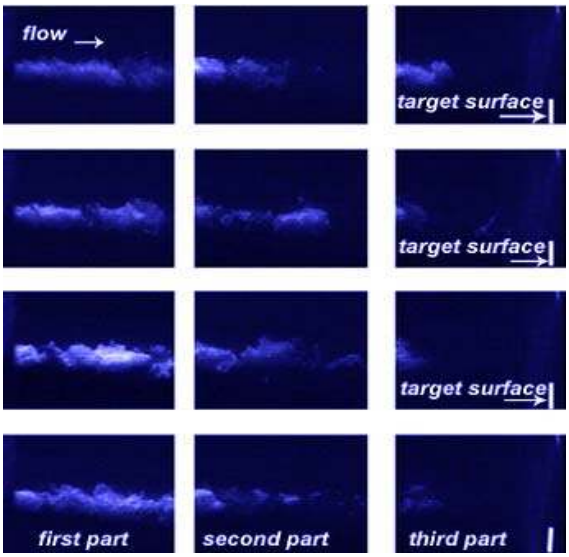

Figure10. Cavitating jet divided in three zones using the magnifier lenses (NAVITAR 2x adapter (1-6010)(1- 6030) (1-60135)). (Shutter time = 1 μs, Gain = 450 V. Conditions: p_1=164 bar, p_2=0.77 bar, v_j =156m/s, σ= 0.0063, T =18°C).

The aim is to show that the cavity bubbles along the jet path collapse anywhere in and around the jet from its starting point until its end. With this technique it is possible to identify where the preferred collapse points are located, and how the location and density of the SL bubbles changed with input parameters, such as cavitation number or jet velocity.

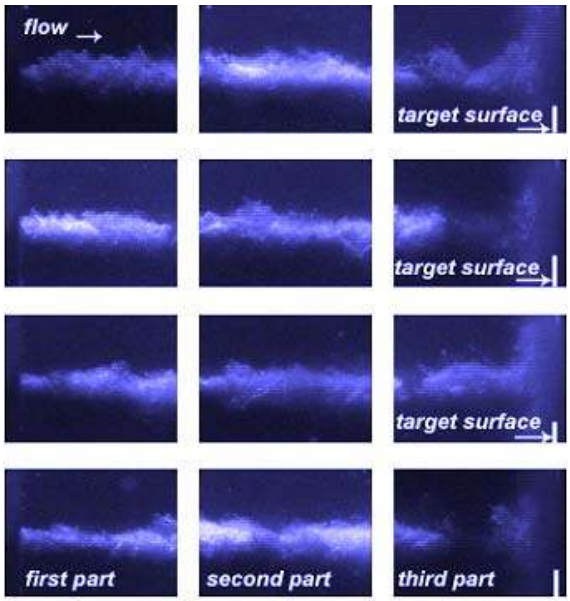

Figure 11. Cavitating jet divided in three zones using the magnifier lenses (NAVITAR 2x adapter (1-6010)(1- 6030) (1-60135)). (Shutter time =1 μs, Gain = 450 V, Conditions: p_1=164 bar, p_2=3.04 bar, v_j=156m/s, σ= 0.025, T =18°C).

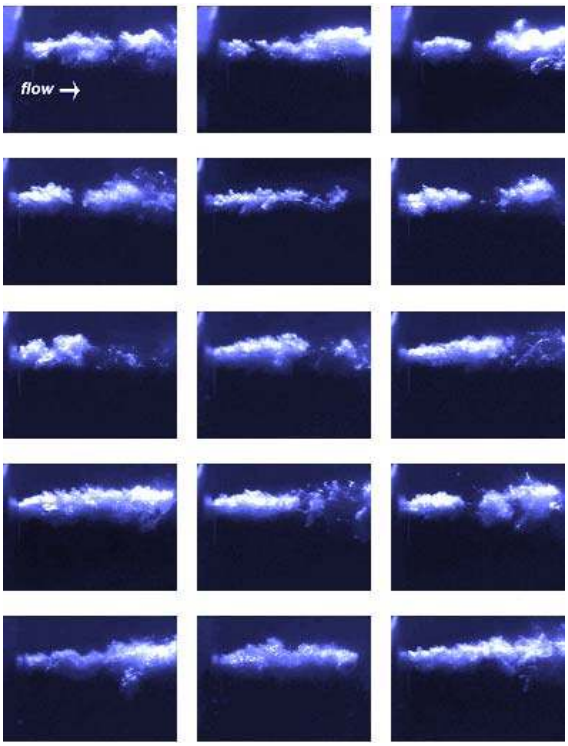

Figure 12. The first part of cavitating jet obtained using NAVITAR system (NAVITAR 2x adapter (1-6010)(1- 6030) (1-60135) magnifier lenses). (Shutter time =1μs, Gain = 600 V. Conditions: p_1=164 bar, p_2=3.04 bar, v_j=156 m/s, σ= 0.025, T = 18°C).

An intensified CCD camera recorded the light emission simultaneously. The intensified camera used (4-QUIK-05) has a standard video output, which can be set to interlaced or non-interlaced operation. The MCP intensifier has a maximum gain of more than 10,000, which should be sufficient to ensure that a recorded photon 'spot' will have a pixel brightness ten units above the noise level in the CCD. The noise level in the CCD typically did not extend above 29 on a scale of 255 brightness levels (the noise level is determined from the image histogram taken while the intensifier is operated at zero gain), so all levels below 29 were rejected. The camera output was recorded by frame grabber software (Matrox Intellicam). Due to the small fraction of emitted photons, which were intercepted by the camera positioned at the working distance from a jet, relatively few SL flashes were recorded in a single superimposed frame.

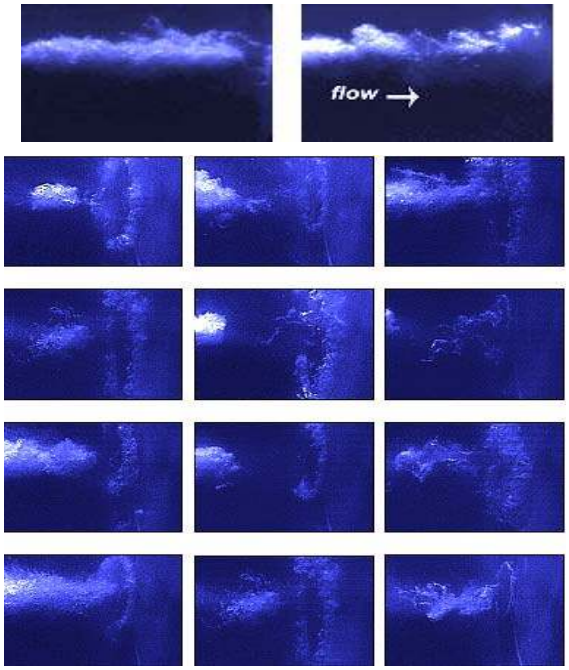

Figure 13. Images of the 2nd and 3rd part of cavitating jet obtained using NAVITAR magnifier lenses (first two images are for the 2nd part) (NAVITAR 2x adapter (1-6010)(1- 6030) (1-60135)). (Gain = 600 V, shutter time = 1 μs, Conditions: p_1=164 bar, p_2=3.04 bar, v_j=156 m/s, σ= 0.025, T =18°C).

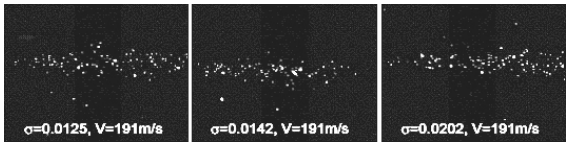

Figure 14. The luminescence phenomenon in a cavitating jet. Flow from left to right. (Conditions: p_1= 213 bar, v_j = 191 m/s, T = 22°C).

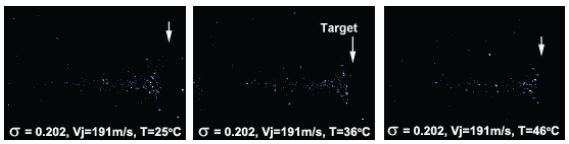

Figure 15. The luminescence phenomenon in a cavitating jet. Flow from left to right. Effect of temperature.

Due to the values of cavitation numbers, there is no clear difference in density of SL spots between the first and the second image in Fig. 14, but the difference exists for the third one. Not all the images obtained using the camera were composed of discrete localised spots of light. Occasionally (once in every few seconds), a comparatively large luminous region would appear in a frame, like in central part of Fig. 14. How these events are to be interpreted is unclear. Perhaps the luminous region was far removed from the focal plane of the camera, or a large cavity or cloud of cavities passed over the SL spot. Another possibility would be that the observed extended luminous regions were actually composed of a large number of individual SL bubbles. The collapse of a cloud of cavitation bubbles, for example, might give rise to the effects recorded.

In Fig.15 the results were obtained at different working fluid temperatures. It was just an attempt to investigate the influence of the temperature on the luminescence density and to see does this phenomenon (existence of spherical bubbles) exist or not when the jet is striking on the specimen surface. Ten pictures were superimposed over each one in Fig.15. The density of photons is decreased as temperature increases. In addition there are some spots or photons along the specimen diameter as a ring.

5. CONCLUSION

Cavitating jet is a phenomenon changeable with time of the order of a μs. The jet appears as white clouds of small bubbles and exhibits a regular frequency of oscillation. The jet behaviour (penetration length, width, etc) depends on the hydrodynamic conditions, such as the cavitation number or p_2 and p_1. When the cavitating jet strikes the wall, the clouds are formed along the surface area producing a jet at the wall and parallel with it. Cavitation rings are produced as a result of such an action. In general, diameter of such rings depends on hydrodynamic conditions and nozzle geometry. The collapsing of bubbles could not be registered because of inadequate temporal resolution of the illuminating and recording system, and a huge number of the bubbles in the cloud cavity (chain production). Observation of the luminescence phenomenon indicates that collapsing of the bubbles takes place everywhere in the jet path. In addition, this also proved the existence of spherical bubbles even for this highly turbulent flow. The kind of visualization system equipment and its resolution is very important to get a good quality of information in the pictures of phenomenon.

Given the experimental data obtained in this study, it should be possible to establish a numerical model as the next logical step.

REFERENCES

[1] Caron, J.F., Farhat, M., Avellan. F.: Physical Investigation of the Cavitation Phenomenon, CAV95, Deauville, France, pp 1-6,1995.

[2] Clanet, C., Lasheras, J.C.: Depth Penetration of Bubbles Entrained by a Plunging Water Jet. Physics Fluids, Vol.9, No.7, pp. 1864-1866, 1997.

[3] Conn, A.F., Johnson, V.E., William, Jr., Lindenmuth, T., Fredrick, G.S.: Some Industrial Applications of Cavitating Fluid Jets Flow, Proceedings of the First U S. Water Jet Conference Golden, Colorado, pp. 338-253, 1981.

[4] Ganippa, L.C, Bark, G., Andersson, S., Chomiak, J.: Comparison of Cavitation Phenomena in Transparent Scaled-Up Single-Hole Diesel Nozzles. CAV2001, California, USA, Session A9.005, june, 2001
(http://cav.2001.library.calteh.edu/)

[5] Ito. Y., Ogata. H., Oba, R., Ikeda, R.: Stereo-Observation of Cavitation Bubbles on a Clark-Y 11.7% Hydrofoil. Trans. ASME, Vol. 54, No 500, Ser. B, pp. 763-769, 1988.

[6] Kato. H., Yamaguchi, H., Maeda, M., Kawanami, Y., Nakasumi, S.: Laser Holographic Observation of Cavitation Cloud on a Foil Section. Journal of Visualization**,** Vol.2, No.1, pp.37-50, July 1999

[7] Keiichi,S., Yasuhiro, S.: Unstable Cavitation Behaviour in a Circular-Cylindrical Orifice Flow, Trans JSME International Journal, Series B, Vol. 45, No. 3, pp.638-645, 2002.

[8] Koivula, T.: On Cavitation in Fluid Power. Proc. of the first FPNI-PhD Symposium, Hamburg 2000, pp. 371-382, 2000.

[9] Oba, R.: The Sever Cavitation Erosion, 2nd International Symposium on Cavitation. Tokyo, Japan, pp. 1-8, 1994.

[10] Soyama, H.: High–Speed Observation of a Cavitating Jet in Air, Trans ASME, Journal of Fluids Engineering, November 2005, Vol. 127, pp. 1095-1101, 2005.

[11] Soyama, H., Adachi, Y., Yamauchi, Y., Oba, R.: Cavitation-Noise-Characteristics Around High Speed Submerged-Water-Jets, Trans. JSME (B), Vol. 60, pp. 730-735,1994.

[12] Soyama, H., Ikohagi, T., Oba, R.: Observation of the Cavitating Jet in a Narrow Watercourse. Cavitation and Multiphase Flow, ASME, FED - Vol. 194, pp. 79-82, 1994.

[13] Soyama, H., Lichtarowicz, A., Lampard D. Useful Correlations for Cavitating Jets. 3rd International Symposium on Cavitation, Grenoble, France, pp. 17-24, 1998.

[14] Soyama, H., Yamauchi, Y., Adachi, Y., Adachi, Y., Oba, R.: High-Speed Cavitation-Cloud Observations Around High-Speed Submerged Water Jets, The second international Symposium on Cavitation, Tokyo, Japan, pp. 225-230, 1994.

[15] Soyama, H., Yamauchi, Y., Adachi, Y., Adachi, Y., Oba, R.: High-Speed Cavitation-Cloud Observations Around High-Speed Submerged Water Jets, Trans JSME International Journal, Series B, Vol.38, No. 2, pp. 245-251, 1995.

[16] Toyoda, K., Muramatsu,Y., Hiramoto, R.: Visualization of the Vortical Structure of a Circular Jet Excited by Axial and Azimuthal Perturbation. Journal of Visualization, Vol.2 No.1, July, pp 17-24,1999.

[17] Vijay, M.M., Zou, C., Tavoularis, S. : A Study of the Characteristics of Cavitating Water Jets by Photography and Erosion, Jet Cutting Technology - Proceedings of the 10th International Conference, pp. 37-67, Elsevier 1991.

[18] Yamauchi, Y., Kawano, S., Soyama, H., Sato, K., Matsudaira, Y., Ikohagi, T., Oba, R.: Formation of process of vortex ring cavitation in high-speed submerged water jet. Trans JSME, ser. B, 62-593; pp. 72-78, 1996.

NOMENCLATURE

σ	cavitation number, $\sigma = \frac{p_{\text{ref}} - p_{\text{v}}}{0.5 \cdot \rho \cdot u_{\text{ref}}^2}$
p_{ref}	reference (downstream) pressure [bar]
$p_{\text{v}}(T)$	saturation (vapour) pressure [bar],
$\rho_{\text{L}}(T)$	density of the liquid [kg/m^3],
T	fluid temperature [^{0}C]
u_{ref}	reference velocity - exit jet velocity [m/s] $u_{\text{ref}} = Q / A = v_{\text{j}}$
q_V	flow rate (m^3/s) $q_V = K \cdot \sqrt{(p_1 - p_2)}$
A	nozzle outlet cross-section area [m^2]
p_1	upstream pressure [bar], (absolute)
p_2	downstream pressure [bar], (absolute)
X	stand-off distance [mm]
L	nozzle length
d_{in} , d_{out}	inlet and outlet nozzle diameter [mm]
K	= 4.78E-09 for divergent ; = 6.17E-09 for convergent nozzle [m^3/s/Pa$^{1/2}$]

ИСТРАЖИВАЊЕ ПОНАШАЊА ПОТОПЉЕНОГ КАВИТАЦИОНОГ МЛАЗА: ПРВИ ДЕО – ФЕНОМЕН, ТЕХНИКА ДЕТЕКЦИЈЕ И СОНО-ЛУМИНЕСЦЕНЦИЈА

Ezddin Ali Farag Hutli, Милош Недељковић

У циљу истраживања и разумевања структуре млаза и понашања кавитационог облака у времену и простору, извршена је визуелизација дубоко потпљеног кавитационог воденог млаза коришћењем камере 4-Quik-05. Ово је захтевало обавезну технику синхронизације и различите типове објектива. Утицај параметара као што су: притисак убризгавања, низводни притисак и кавитацијски број, и њихов значај је експериментално доказан. Записи сонарно-луминесцентног феномена су потврдили да мехурови нестају дужином читаве путање млаза. Такође, истраживан је и ефекат утицаја температуре на звучну-луминесценцију.